Wave Chaos in Real-World Vertical-Cavity Surface-Emitting Lasers

Tobias Gensty,[1,*] Klaus Becker,[1] Ingo Fischer,[1] Wolfgang Elsäßer,[1] Christian Degen,[2]
Pierluigi Debernardi,[3] and Gian Paolo Bava[3]

[1]*Institute of Applied Physics, Darmstadt University of Technology, Schloßgartenstraße 7, 64289 Darmstadt, Germany*
[2]*Infineon Fiber Optics GmbH, Otto-Hahn-Ring 6, 81739 München, Germany*
[3]*Istituto di Elettronica e di Ingegneria dell'Informazione e delle Telecomunicazioni, Politecnico di Torino e Istituto Nazionale per la Fisica della Materia, Unità di Ricerca di Torino, Corso Duca degli Abruzzi, 24, 10129 Torino, Italy*

(Received 14 October 2004; published 13 June 2005)

We report the onset of wave chaos in a real-world vertical-cavity surface-emitting laser. In a joint experimental and modeling approach we demonstrate that a small deformation in one layer of the complicated laser structure changes the emission properties qualitatively. Based on the analysis of the spatial emission profiles and spectral eigenvalue spacing distributions, we attribute these changes to the transition from regular behavior to wave chaos, and justify the full analogy to two-dimensional billiards by model calculations. Hence, these lasers represent fascinating devices for wave chaos studies.

DOI: 10.1103/PhysRevLett.94.233901 PACS numbers: 42.65.Sf, 05.45.Mt, 42.55.Px

Quantum chaos terms phenomena corresponding to classically chaotic behavior in the semiclassical limit. It can be studied in quantum systems, but also in electromagnetic resonators—then termed "wave chaos"—due to the isomorphism of the Schrödinger and Helmholtz equation in two dimensions. Generic fingerprints of chaos have proven to exist, e.g., in the eigenvalue distributions, depending on integrable or nonintegrable boundary conditions, corresponding to regular or chaotic behavior, respectively. Such characteristics have been widely studied in microwave billiards [1–3]. In optical resonators, wave chaos has been predicted for semiconductor microdisk lasers [4,5]. The first experimental results of the investigations on microdisk lasers are in agreement with the theoretical predictions [6,7]. Huang *et al.* [8] concluded from a phenomenological comparison of the mode patterns and the wave functions of two-dimensional billiards that vertical-cavity surface-emitting lasers (VCSEL) could be interpreted as two-dimensional billiard systems, and they suggested that large-aperture VCSELs might be appropriate systems for wave chaos studies. Here, we report the experimental observation of wave chaos in real-world VCSELs as being used in data-communication applications. Furthermore, we justify the full analogy between VCSELs and two-dimensional billiards by model calculations.

VCSELs are modern sophisticated semiconductor laser structures that have become standard lasers in optical data communication, thus being important technological systems. Furthermore, because of their small size, particular structure, and geometry, they are of tremendous interest for fundamental physics studies [9–12]. The lasers in our experiments are oxide-confined VCSELs emitting at a wavelength of $\lambda \approx 850$ nm. Figure 1(a) depicts a schematic sketch of a VCSEL. The active layer of the laser is placed between two distributed Bragg reflectors (DBR), establishing the cavity, with reflectivities of 99.7% for the top mirror and 99.9% for the bottom mirror, respectively. The distance between the top and bottom DBR is one wavelength, resulting in the desired longitudinal single mode behavior. Nevertheless, the laser emission is likely

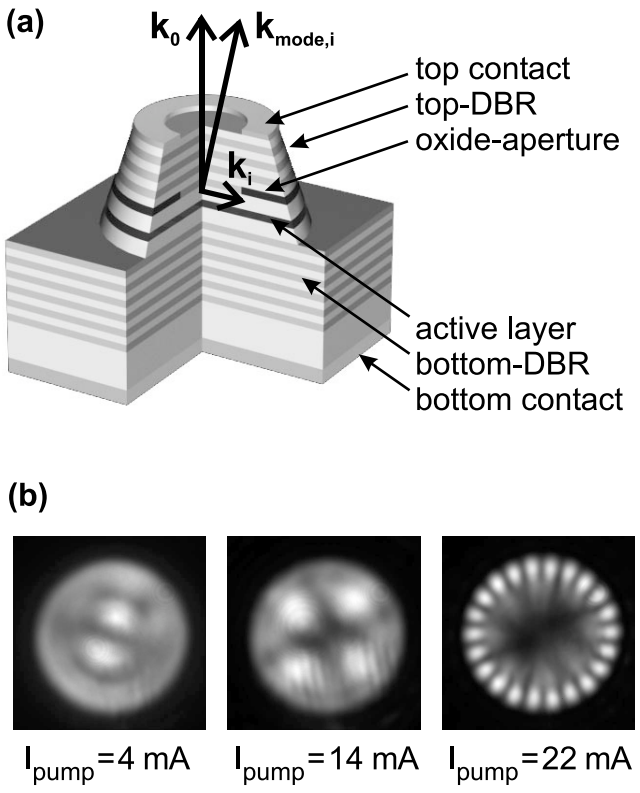

FIG. 1. (a) Schematic sketch of a VCSEL with a circular oxide aperture. Also indicated is the wave vector of the *i*th transverse mode $\mathbf{k_{mode,i}}$ as well as its longitudinal $\mathbf{k_0}$ and transverse component $\mathbf{k_i}$. (b) Experimentally determined intensity distributions for three different pump currents of a VCSEL with a circular oxide aperture.

to exhibit many transverse modes due to the broad area of the active region compared to the product of the wavelength and the length of the cavity, a characteristic quantity known as the Fresnel number. For these VCSELs, the Fresnel number is in the order of $F \sim 160$. For transverse confinement an oxide aperture is incorporated into the top DBR. This oxide aperture acts as current confinement and defines an optical waveguide (index guiding), since the difference of the refractive index of the semiconductor material and the surrounding oxide is very high ($\Delta n \sim 2$), thus defining the transverse resonator shape. It is fabricated by a selective wet oxidation process of a layer of AlAs. The light inside the cavity propagates normal to the plane of the semiconductor layers. The emission occurs through the aperture defined by the top electrical ring contact. The emitted light is linearly polarized in two orthogonal polarization directions, which in the following is denoted as 0° and 90° polarization, respectively. The 0.3% outcoupled laser emission through the top mirror allows direct visualization of the two-dimensional intensity distribution inside the cavity by performing a single lens projection onto a CCD camera. Figure 1(b) depicts the 0° polarization intensity distributions of a VCSEL incorporating a circular oxide aperture with 14 μm in diameter for three different pump currents, $I = 4$, 14, and 22 mA, while the laser threshold current is $I_{\text{th}} = 2.3$ mA. The corresponding intensity distributions can be identified as Gauss-Laguerre ($LG_{r,\phi}$) modes, in particular, the $LG_{2,1}$, $LG_{0,2}$, and $LG_{0,11}$ modes, respectively. The parameters r and ϕ denote the radial and azimuthal mode indices, respectively [13]. The LG modes represent the mathematical solutions of a cavity with a cylindrical symmetry. From this, we conclude that this VCSEL, indeed, incorporates a circular oxide aperture which defines the shape of the resonator. However, the technological fabrication process of the VCSELs can be performed such that a deformed shaped aperture, rather than a circularly shaped one, is realized, because the oxidation rate depends on the crystallographic axes [14]. The second VCSEL in our experiments exhibits an elongated, deformed aperture shape with principal axes of 13 and 15 μm in diameter, respectively. The deformation of the oxide aperture can be deduced from the shapes of the emission profiles, depicted in Fig. 2 for three different pump currents, $I = 15$, 20, and 30 mA, respectively. Here, the threshold current is $I_{\text{th}} = 2.5$ mA. The top row depicts the 90° polarization (along the shorter principal axis) and the bottom row the 0° polarization. The emission of this VCSEL does not exhibit LG modes as in the case of the VCSEL with the circular oxide aperture (cf. Fig. 1(b)]. Instead, in Fig. 2, we find characteristic intensity profiles commemorating classical particle trajectories, known as scars [15,16]. The intensity distribution of the 90° polarization for $I = 15$ mA displays, e.g., a clear bow-tie profile. For $I = 20$ mA a whispering gallery–like mode can be recognized. The distribution of the 0° polarization for $I = 30$ mA shows a horizontally directed bouncing-ball mode. Such scars can be regarded as indicators of wave chaos [17]. Thus, the deformation from the circular aperture shape to the elongated, deformed one not only results in different intensity distributions, but also qualitatively changes the basic physical properties of the VCSEL. This indicates a transition from a regular to a chaotic system.

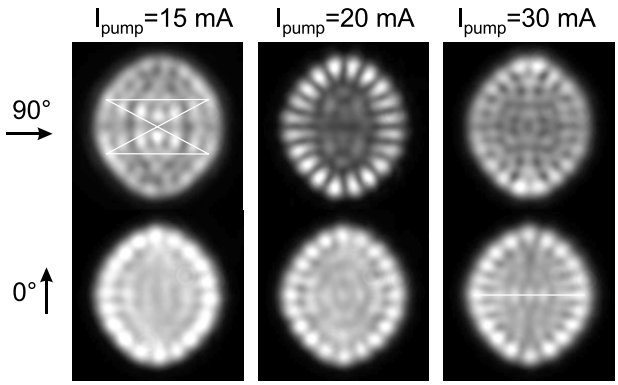

FIG. 2. Polarization resolved intensity distributions of the VCSEL with the deformed aperture shape for three different pump currents. The top row depicts the 90° polarization direction, which is along the shorter principal axis, and the bottom row depicts the 0° polarization direction. The white lines indicate scars of classical particle trajectories.

In order to support this hypothesis, we analyze the optical spectra of the laser emission of the VCSELs via cumulated eigenvalue spacing distributions $P(s)$ which are derived from the nearest-neighbor eigenvalue spacing distributions $\tilde{p}(s)$. The nearest-neighbor eigenvalue spacing distribution obeys a Poisson distribution $\tilde{p}(s) = \exp(-s)$ for a regular system and a Wigner distribution $\tilde{p}(s) = \frac{1}{2}\pi s \exp(-\frac{1}{4}\pi s^2)$ for a chaotic system. The normalized mode spacing parameter s is defined as

$$s_i = \frac{(E_i - E_{i-1})}{\langle E \rangle}, \tag{1}$$

with E_i denoting the normalized energy of the ith eigenmode and $\langle E \rangle$ the mean energy spacing. The cumulated eigenvalue spacing distribution $P(s)$ is defined as

$$P(s) = \int_0^s \tilde{p}(s')ds', \tag{2}$$

where $\tilde{p}(s)$ is the probability density of the nearest-neighbor eigenvalue spacing distribution. Since we are interested in the analogy between a wave with wave vector $\mathbf{k}$ and the chaotic trajectory of a corresponding classical particle, we define the normalized energy of the wave as the normalized energy of a corresponding quantum mechanical particle, $E_i \sim k_i^2$, where k_i is the transverse wave number of the optical mode given by [cf. Fig. 1(a)]

$$k_i^2 = k_{\text{mode},i}^2 - k_0^2, \tag{3}$$

where $k_{\text{mode},i}$ is the wave number of the ith transverse mode

and k_0 denotes its longitudinal component. In this case, k_0 is also the wave number of the fundamental Gaussian mode. Therefore, we have recorded highly resolved optical spectra of the laser emission for both VCSELs at $I = 20$ mA with a resolution of better than 6 GHz. Because of the large Fresnel number, the lasers exhibit 84 and 65 modes within the optical spectra of the dominant 0° polarization of the VCSELs with the circular and the deformed oxide apertures, respectively. For comparison with the experimental data, we have calculated the corresponding distribution functions by numerically generating two eigenvalue spectra each comprising 5000 eigenmodes based on the Poisson distribution for a regular system and on the Wigner distribution for a chaotic system, respectively. Then, we have analyzed the mode spacings step by step merging all modes which were below the resolution limit of 6 GHz. Finally, we have calculated the resulting truncated cumulated spacing distributions which are depicted in Fig. 3 for reference to the experimental results. Figure 3(a) depicts the experimentally determined cumulative eigenvalue spacing distribution of the VCSEL with the circular oxide aperture. We find excellent agreement of the experimentally obtained distribution with the truncated integrated Poisson distribution. In contrast, the cumulative eigenvalue statistics of the VCSEL incorporating the elongated, deformed oxide aperture is much closer to the integrated Wigner distribution, also known as the Gaussian orthogonal ensemble (GOE) statistics as can be seen from Fig. 3(b). The GOE statistics is the characteristic distribution of a chaotic system [3]. Thus, this analysis supports the analogy between the circular shaped oxide-aperture VCSEL and an electromagnetic billiard with integrable boundary conditions defining a regular system, whereas the deformed shaped oxide-aperture VCSEL behaves like a billiard with nonintegrable boundary conditions resulting in the onset of wave chaos in the VCSEL resonator.

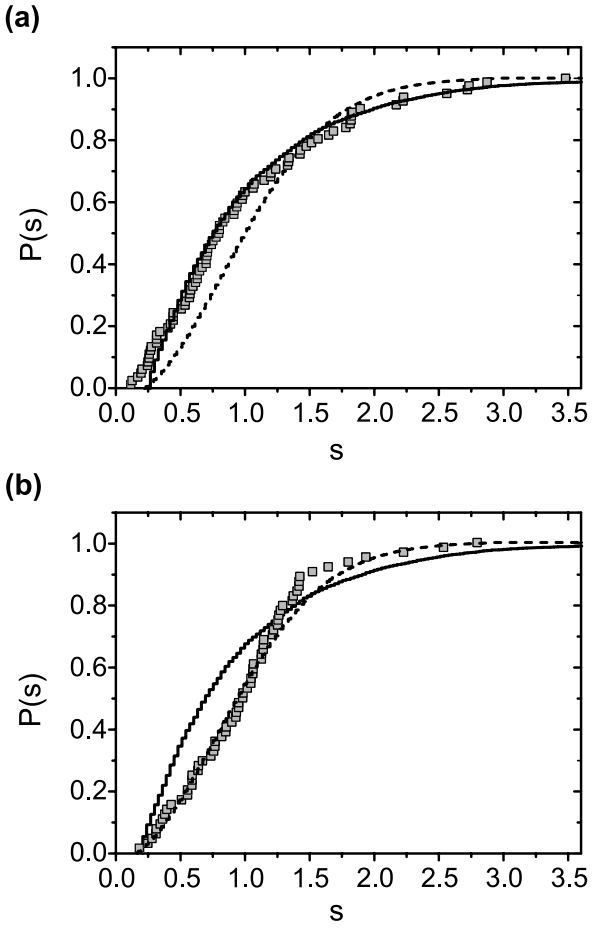

FIG. 3. Experimentally obtained cumulated eigenvalue spacing distributions and corresponding reference distributions. The experimental distributions (symbols) are derived from the optical spectra of the VCSELs with the (a) circular and (b) deformed aperture shapes. The curves represent truncated integrated Poisson distributions (solid line) for a regular system, and the resolution limited GOE statistics (dashed line) for a purely chaotic system. The mean mode spacing of $s = 1$ refers to an optical mode spacing of (a) 20.5 GHz and (b) 25.5 GHz, respectively.

The remaining key question is the following: In how far is it actually justified to interpret the emission characteristics of such a complicated three-dimensional laser structure in terms of a simple two-dimensional billiard or resonator? In order to clarify this fundamental point, we have performed model calculations based on a three-dimensional vectorial model [18] which has proven to be suitable to quantitatively derive the eigenmodes, the corresponding frequencies, and the modal threshold gain for such VCSELs [19,20]. We have performed the modeling for a circularly shaped oxide aperture with a radius r_0 and for a quadrupolarly deformed oxide aperture ($r(\varphi) = r_0[1 + 0.205\cos(2\varphi)]$ in polar coordinates), which is known to be a chaotic system in pure two dimensions [21]. In both simulations, r_0 has been chosen to be $r_0 = 7\ \mu$m. In order to obtain well-defined cumulative eigenvalue spacing distributions, we have decomposed the symmetries of our investigated systems. Only those modes have been analyzed that have nodal lines along the boundaries of the gray shaded areas (Fig. 4, insets). The reduction of one symmetry axis in the case of the circular oxide aperture avoids the degeneracy of eigenmodes from the VCSEL model due to the symmetry of the system. In the case of the quadrupolarly deformed aperture shape, the symmetry decomposition to a single symmetry class is essential in order to obtain the generic GOE statistics [22–24]. We have found 199 modes for the circularly shaped oxide aperture and 101 for the quadrupolarly deformed aperture, respectively. The obtained cumulated eigenvalue spacing distributions are depicted in Fig. 4. Remarkably, we get excellent agreement with an integrated Poisson distribution in the case of the circular aperture and with a GOE statistics in the case of the quadrupolarly deformed aperture, respectively. Thus, the spatial and spectral emission properties of the VCSELs are, indeed, determined by the shape of their oxide aperture, behaving

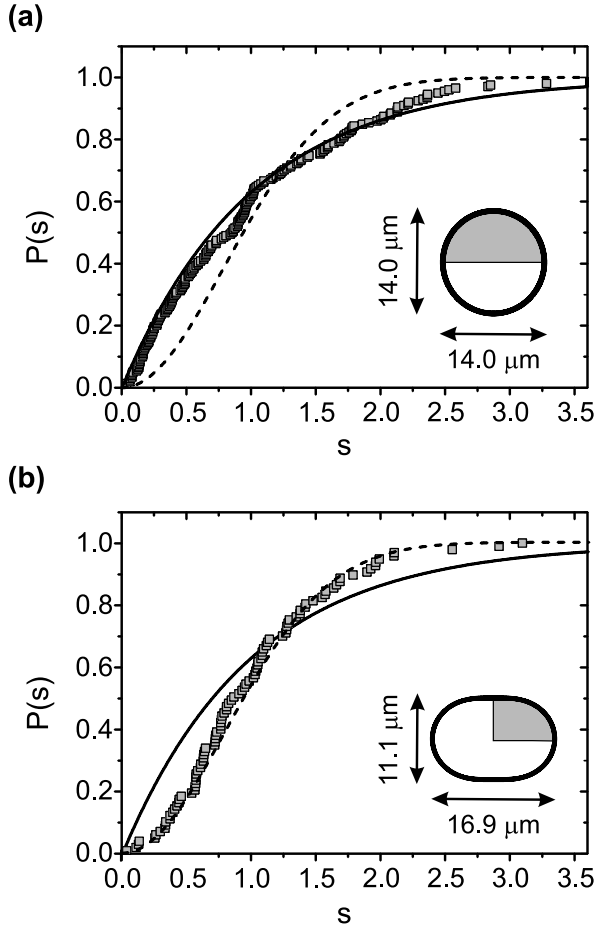

FIG. 4. Cumulated eigenvalue spacing distributions obtained from modeling and corresponding reference distributions. The modeled distributions (symbols) are obtained for VCSELs incorporating a (a) circularly and (b) quadrupolarly deformed aperture shape. The solid lines represent an integrated Poisson distribution for a regular system and the dashed lines a GOE statistics for a purely chaotic system. The insets show the aperture shapes of the investigated systems.

completely like two-dimensional billiards. In particular, the calculations confirm our experimentally obtained results that wave chaos appears in VCSELs, if nonintegrable boundary conditions are defined by the oxide aperture.

In conclusion, our joint experimental and theoretical approach leads to a clear identification of wave chaos in a complicated real-world laser resonator. We have demonstrated that a deformation of the oxide aperture results in qualitative changes of the emission properties. We have observed Gauss-Laguerre modes in the emission profiles of a VCSEL with circular oxide aperture, and scar modes in the emission profiles of the VCSEL with the deformed oxide aperture. Based on the analysis of the eigenvalue spacing distributions, we attribute these changes to the onset of wave chaos in a two-dimensional billiard and justify our interpretation via model calculations. These insights promise further stimulating wave chaos studies in VCSELs and open perspectives for their technological consideration. Even beneficial exploration could be aspired.

We thank A. Barchanski for helpful calculations on microwave billiards.

*Electronic address: tobias.gensty@physik.tu-darmstadt.de

[1] H.-J. Stöckmann and J. Stein, Phys. Rev. Lett. **64**, 2215 (1990).
[2] H.-D. Gräf, H. L. Harney, H. Lengeler, C. H. Lewenkopf, C. Rangacharyulu, A. Richter, P. Schardt, and H. A. Weidenmüller, Phys. Rev. Lett. **69**, 1296 (1992).
[3] H.-J. Stöckmann, *Quantum Chaos—An Introduction* (Cambridge University Press, Cambridge, 1999).
[4] J. U. Nöckel and D. Stone, Nature (London) **385**, 45 (1997).
[5] T. Harayama, P. Davis, and K. S. Ikeda, Phys. Rev. Lett. **90**, 063901 (2003).
[6] C. Gmachl, F. Capasso, E. E. Narimanov, J. U. Nöckel, A. D. Stone, J. Faist, D. L. Sivco, and A. Y. Cho, Science **280**, 1556 (1998).
[7] T. Harayama, T. Fukushima, P. Davis, P. O. Vaccaro, T. Miyasaka, T. Nishimura, and T. Aida, Phys. Rev. E **67**, 015207(R) (2003).
[8] K. F. Huang, Y. F. Chen, H. C. Lai, and Y. P. Lan, Phys. Rev. Lett. **89**, 224102 (2002).
[9] K. J. Vahala, Nature (London) **424**, 839 (2003).
[10] H. Pier, E. Kapon, and M. Moser, Nature (London) **407**, 880 (2000).
[11] L. Fratta, P. Debernardi, G. P. Bava, C. Degen, J. Kaiser, I. Fischer, and W. Elsäßer, Phys. Rev. A **64**, 031803(R) (2001).
[12] P. G. Savvidis, J. J. Baumberg, R. M. Stevenson, M. S. Skolnick, D. M. Whittaker, and J. S. Roberts, Phys. Rev. Lett. **84**, 1547 (2000).
[13] A. E. Siegman, *Lasers* (University Science Books, Mill Valley, CA, 1976).
[14] K. D. Choquette, K. M. Geib, H. C. Chui, B. E. Hammons, H. Q. Hou, and T. J. Drummond, Appl. Phys. Lett. **69**, 1385 (1996).
[15] P. Wilkinson, T. Fromhold, L. Eaves, F. Sheard, N. Miura, and T. Takamasu, Nature (London) **380**, 608 (1996).
[16] E. J. Heller, Phys. Rev. Lett. **53**, 1515 (1984).
[17] J. Stein and H.-J. Stöckmann, Phys. Rev. Lett. **68**, 2867 (1992).
[18] G. P. Bava, P. Debernardi, and L. Fratta, Phys. Rev. A **63**, 023816 (2001).
[19] P. Debernardi, G. P. Bava, C. Degen, I. Fischer, and W. Elsäßer, IEEE J. Quantum Electron. **38**, 73 (2002).
[20] C. Degen, I. Fischer, W. Elsäßer, L. Fratta, P. Debernardi, G. P. Bava, M. Brunner, R. Hövel, M. Moser, and K. Gulden, Phys. Rev. A **63**, 023817 (2001).
[21] A. D. Stone, Physica (Amsterdam) **288A**, 130 (2000).
[22] M. V. Berry and M. Robnik, J. Phys. A **17**, 2413 (1984).
[23] R. Schäfer, M. Barth, F. Leyvraz, M. Müller, T. H. Seligman, and H.-J. Stöckmann, Phys. Rev. E **66**, 016202 (2002).
[24] C. Dembowski, H.-D. Gräf, A. Heine, H. Rehfeld, A. Richter, and C. Schmit, Phys. Rev. E **62**, R4516 (2000).